A Study on Development of the Three-Dimensional Numerical Model to Analyze the Casting Process : Mold Filling and Solidification

Jinho Mok*

Nano Cast Korea,
Gojan-dong, Namdong-gu, Inchon 257-42, Korea

A three dimensional model was developed to analyze the mold filling and solidification in the casting processes. The model uses the VOF method for the calculation of the free surface and the modified Equivalent Specific Heat method for the treatment of the latent heat evolution. The solution procedure is based on the SIMPLER algorithm. The complete model has been validated using the exact solutions for phase change heat transfer and the experimental results of broken water column. The three-dimensional model has been applied to the benchmark test and the results were compared to those from experiment, a two-dimensional analysis, and another three dimensional numerical model.

Key Words : Mold Filling, Solidification, Free Surface, Phase Change, SIMPLER, VOF, Equivalent Specific Heat

Nomenclature

α	: Thermal diffusion coefficient
a	: coefficients for discretized equations
A	: Area
b	: Source term
C_f	: Wall friction variation
c_p	: Specific heat
D_h	: Hydraulic diameter
f	: Fraction
F	: Volume fraction
Φ	: Dependent variable
Γ	: Diffusion coefficient
g	: Gravitational force
h	: Heat transfer coefficient
ΔH	: Release of latent heat
k	: Thermal conductivity
L	: Latent heat
Λ	: Darcy friction factor
p	: Pressure
q	: Heat flux
R	: Thermal resistance
ρ	: Density
S, S_c, S_p	: Linearized source term
t	: Time
T	: Temperature
T_p	: Initial temperature
T_f	: Interface temperature
τ_w, τ	: Shear stress
u, v	: Velocity components
V	: Volume
x, y, z	: Index for Cartesian coordinate

Subscripts

A, D, AD	: Acceptor, donor, interface
av	: Average
i, p, e, w, n, s, t, b	: Directions
nb	: Neighbor
s, l, m	: Solid, liquid, mold
sol, liq	: Ssolidus, liquidus

Superscripts

$n, n+1$	: Previous (or present) and the next time stage
old	: Previous (or present) time stage

* E-mail : mokjinho@yonsei.ac.kr
TEL : +82-2-2123-2837; FAX : +82-23-3147-2641
Nano Cast Korea, Gojan-dong, Namdong-gu, Inchon 257-42, Korea. (Manuscript **Received** October 21, 2004; **Revised** April 126, 2005)

1. Introduction

Casting is widely used for manufacturing materials that possess the characteristics of fluidity and solidification. The presence of the free surface and the phase-change interface, however, causes numerous defects in the final products. In addition, since the process is done under the environment of extremely high temperature, it is almost impossible to observe the interim process inside the material. Consequently, significant trial and error is required to produce defect-free products. With recent advances in numerical methods and physical models, computer modeling has become an attractive tool for mold design. However, the presence of free surface and phase-change front makes the numerical solution very unstable and leads to severe convergence difficulties, especially for three-dimensional flows. The development of MAC (Marker And Cell), SMAC (Simplified Marker And Cell), and SOLA-VOF (SOLution Algorithm for transient fluid flow — Volume Of Fluid) promoted the researches on the simulation of mold flows both quantitatively and qualitatively. Most of the existing models for free surface tracking in mold filling are based on the SMAC or the SOLA algorithm (Harlow et al., 1971 ; Hirt et al., 1968, 1981 ; Hwang et al., 1983 ; Nichols et al., 1971), while the SIMPLE algorithm and variants (Patankar, 1980), which are widely used in modeling of fluid flow and heat transfer in other industries including the simulations of solidification process to predict the phase change front behavior or the segregation phenomena (Bennon et al., 1987a, 1987b ; Lee et al., 1995, 2001), have been adopted by a relatively few investigators for modeling casting processes (Bennon et al., 1987a, 1987b ; Hong et al., 2001 ; Lee et al., 1999). It is because that the time step limitation is inevitable to trace the free surface and, as a result, the explicit schemes (MAC, SMAC, SOLA-VOF etc. are on the explicit scheme basis) perform much faster calculation than the implicit schemes (SIMPLE, SIMPLER etc. are on the implicit scheme basis) at the same time step. The solution algorithms used in

the SMAC and SOLA-VOF are nicely implemented based on the explicit scheme so that they can be combined with MAC (Marker And Cell) method and the VOF (Volume Of Fluid) method. These days, the phase change heat transfer is considered in SMAC or SOLA-VOF via the Temperature Recovery method, the Equivalent Specific Heat method, or the Enthalpy method. There have also been continuous efforts to solve the free surface flow adopting implicit numerical schemes. Lee et al. combined the SIMPLE algorithm with the MAC method and analyzed a two dimensional filling process (Lee et al., 1999), but the MAC method is hardly expanded to the three dimensional model due to memory trouble. Koo et al. analyzed the centrifugal casting process by combining the SIMPLE algorithm and VOF method to deal with centrifugal force stably (Koo et al., 2001), but the free surface was not treated as a transient phenomenon but assumed to be in the steady state. Hong et al.'s mold filling model combined the SIMPLE algorithm with the VOF method based on the BFC (Body Fitted Coordinate) system (Hong et al., 2001) and Mampaey et al.'s adopted the non-orthogonal meshes for the accurate and effective calculations (Mampaey et al., 1995). But both of them care only for the filling process of curved thin walled castings. Hetu et al. simulated the mold filling and solidification processes adopting FEM (Hetu et al., 1999), but it usually takes more computational memory and calculation time compared to the FDM or FVM due to more simultaneous equations to be solved. Besides memory and computation time, the combined effect of diffusion and convection on transport phenomena is more effectively treated in FDM or FVM than FEM by the Hybrid scheme or the Power Law scheme. But because of nice fitting along the boundary, still the BFC or FEM approach is very useful method in the simulations of thin and curved cavity filling.

As mentioned already, the SIMPLE algorithm is an implicit scheme, while most free surface tracking techniques are based on the explicit concept. Even though the implicit schemes are adopted for the mold flows combined with the MAC or

VOF method, still there exist limitations on the time steps. If the same time steps is applied to, the explicit schemes are more effective method than the implicit schemes because the explicit schemes do not solve the simultaneous equations but just substitute the values of previous time stage (Φ^n) into the discretized equations to get the values for next time stage (Φ^{n+1}): $\Phi^{n+1} = f(\Phi^n)$. But the casting processes consist not only of filling process but also of solidification process. And because of the latent heat release, it takes much more time for solidification than for filling, physically. And if the explicit approach is to be applied continuously even after the completion of filling, it will take too much time to finish the calculation of solidification due to the limitation of time steps imposed by the explicit method : that is, in the explicit method, the time step must not exceed a specific value for stable calculation and convergence, whose value is getting smaller according to the smaller mesh size, larger diffusive coefficients, and stronger convection. On the other hand, there isn't any restrictive condition on time step in the implicit method. So if the whole casting process (from filling to final solidification) is to be simulated, the implicit approach saves much time comparing to the explicit method since we can save computation time finishing the calculation of solidification which takes much longer time physically (and as a result, much more iteration numbers computationally) than filling process. In addition, an implicit scheme is very useful to treat the various body forces in the casting processes based on its stable discretized equations, while an explicit scheme hardly copes with the body forces like Darcian damping, centrifugal force, turbulent properties, etc.

Those motivated the present research to develop a combined model for casting processes. This model is based on the SIMPLER algorithm (Patankar, 1980), accounts for three-dimensional effects, and includes all processes : from filling to final solidification. The model has been validated using the exact solution of a simple problem involving phase change (Ohnaka, 1984) and the experimental results for the collapse of a water column (Hetu et al., 1999). Finally, the present

numerical model has been applied to the bench mark test (Sirrell et al., 1995) and the results have been compared with the experimental results, a two dimensional numerical results, and the other three dimensional numerical results to highlight its exact prediction.

2. Numerical Analysis

2.1 Basic equations and boundary conditions

The casting processes include several physical phenomena. Like other CFD problems, the casting process requires the solution of the continuity equation, the momentum equation, and the energy equation. In addition, the modeling of casting process requires treatment of free surface and phase change. The free surface is treated via the volume of fluid (VOF) method, which requires solutions of equation for volume fraction. The phase change process is modeled using the modified Equivalent Specific Heat method. The aforementioned partial differential equations can be represented in a generalized form as Eq. (1). This equation contains four terms. These are, from left to right, the unsteady term, the convection term, the diffusion term, and the source (or sink) term. Individual equations can be recovered from Eq. (1) by assigning specific meanings to Φ, Γ, and S (see Table 1).

Table 1 Definitions of Φ, Γ, and S in Eq. (1)

	Φ	Γ	S
Continuity Equation	1	0	0
Volume Fraction	F	0	0
Momentum Equation (velocity)	u	μ	$-\partial p/\partial x$
	v	μ	$-\partial p/\partial y + \rho g$
	w	μ	$-\partial p/\partial z$
Energy Equation (temperature)	T	k/c_p	$\rho/c_p \cdot (\partial \Delta H/\partial t)$

μ : Dynamic viscosity k : Thermal conductivity
c_p : Specific heat ρ : Density
ΔH : Evolution of latent heat

$$\frac{\partial}{\partial t}(\rho \Phi) + \frac{\partial}{\partial x_i}(\rho u_i \Phi) = \frac{\partial}{\partial x_i}\left(\Gamma \frac{\partial \Phi}{\partial x_i}\right) + S \quad (1)$$

No slip wall boundary condition is applied at the mold walls. At the free surface, the normal and tangential stress conditions were applied (Hirt et al., 1968 ; Nichols et al., 1971) : that is, the normal stress is balanced by the pressure on the free surface and there is 0-shear stress on it. The accuracy of the free surface motion depends on the correct satisfaction of the normal and the tangential stress conditions. The wall boundary condition and the free surface boundary conditions (normal and tangential stress conditions) can be expressed as :

No slip wall boundary condition

$$u_i = 0 \quad (2)$$

Normal stress condition

$$p_{free-surface} = \delta_{ij}\sigma_{ij} + p_{appliec}, \quad (3)$$
$$\delta : \text{Kronecker delta}$$

Tangential stress condition

$$\tau_{ij} = 0 \quad (i \neq j) \quad (4)$$

For heat transfer through each boundary (cast-inner air, cast-mold, mold-coolant or outer air), thermal resistance circuits are constructed and the effective heat transfer coefficients are calculated (Mills, 1992 ; Patnakar, 1980).
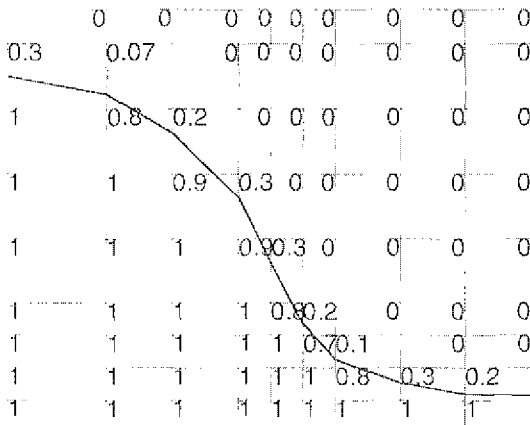
2.2 Numerical method

The basic SIMPLE algorithm is well known and is not described here : details are available in (Patankar, 1980). In this section, details are given for the Volume of Fluid (VOF) method for calculating the free surface, the modified Equivalent Specific Heat method for calculating the latent heat release, and the boundary conditions. The VOF method is based on the explicit scheme, whereas the SIMPLE algorithm is based on the implicit scheme. To save the calculation time during filling process analysis, the PBP (Point By Point) method is to be used for velocity field calculation instead of the LBL (Line By Line) method (Hong et al., 2001 ; Patnakar, 1980). It's to avoid including velocity calculation in the mold and empty zones.
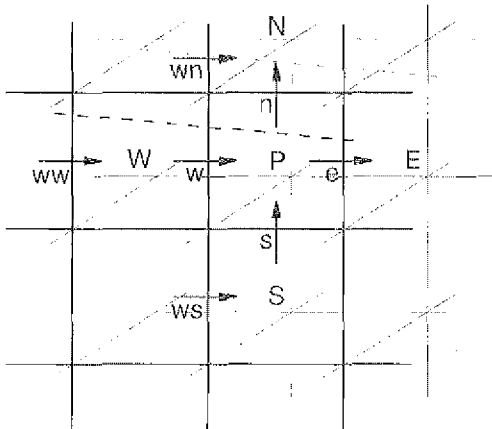
2.2.1 Free surface tracking

The VOF method, adopted in the present combined algorithm, is one of the widely used methods to track the free surface (Hirt et al., 1981 ; Hong et al., 2001 ; Nichols et al., 1971). Formation of free surface is interpreted as a transport phenomenon of volume fraction of fluid. It is governed by the volume fraction advection equation, and volume fraction is transferred only by convection, that is $\Gamma = 0$ as in Table 1. So each control volume has a volume fraction of fluid whose value is between 0 and 1 as a result of solving volume fraction equations, as it has its own value of temperature or velocity. The control volume includes free surface and is classified as a free surface cell, when the volume fraction is less than 1 and lager than 0 (1 : fully fluid cell, 0 : empty cell). One example of free surface tracking according to volume fraction of fluid is shown in Fig. 1(a). The discretized volume fraction equation can be written as (see Fig. 1(b), (c) as well) :

$$F_P = F_P^{old} - \frac{\Delta t}{\Delta x_P}(u_e^{old}F_e^{old} - u_w^{old}F_w^{old})$$
$$- \frac{\Delta t}{\Delta y_P}(v_n^{old}F_n^{old} - v_s^{old}F_s^{old}) \quad (5)$$
$$- \frac{\Delta t}{\Delta z_P}(w_t^{old}F_t^{old} - w_b^{old}F_b^{old})$$

where the superscript old denotes the previous time stage value. The 4th term in the right hand side is the extended form for the three dimensional analysis. Other symbols are explained in Fig. 1(b), (c). $u_e^{old} \cdot F_e^{old}$, $u_w^{old} \cdot F_w^{old}$, ··· are defined in the boundaries of adjacent two cells and their values are determined by the Donor and Accepter Flux Approximation method (Hirt et al., 1981). (Illustration in Fig. 1(b) is a two dimensional situation for the better look and easier understanding.) Assume the adjacent two cells (control volumes) are P and E as in Fig. 1(b), one will be a donor cell and another an accepter cell according to the sign of ue the velocity at the interface of P and E : if u_e is negative value (from E to P), cell E is a Donor and cell P is an Accepter. And then the amount of volume fraction of fluid transferred from a donor to an

```
0     0    0 0 0 0    0    0    0
0.3   0.07 0 0 0 0    0    0    0
1     0.8  0.2  0 0 0 0    0    0
1     1    0.9  0.3 0 0 0    0    0
1     1    1    0.9 0.3 0    0    0
1     1    1    1  0.8 0.2   0    0
1     1    1    1  1  0.7 0.1  0    0
1     1    1    1  1  1  0.8 0.3 0.2
1     1    1    1  1  1    1    1
```

(a) Free surface tracking by volume fraction value

(b) Grid system with one example of free surface boundary
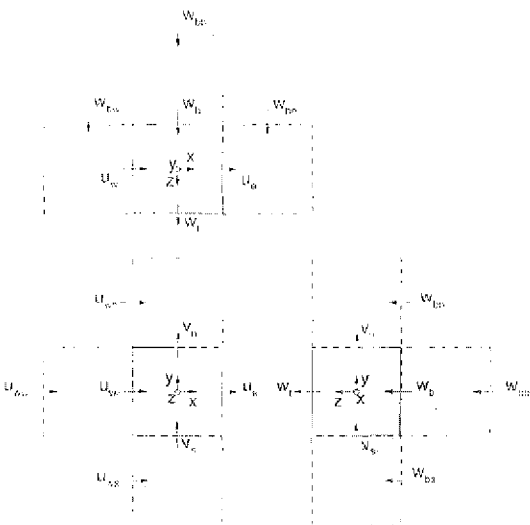
(c) Three dimensional situation of control volume P

Fig. 1 Boundary examples for free surface tracking

accepter can be determined depending on the volume fraction of fluid in the donor and accepter. There are two different cases in the volume fraction values of donor and accepter : they are $F_D \cdot \Delta x_D \geq F_A \cdot \Delta x_A$ and $F_D \cdot \Delta x_D < F_A \cdot \Delta x_A$, where $F_A \cdot \Delta x_A = F_{AD} \cdot u_{AD} \cdot \Delta t$. If $F_D \cdot \Delta x_D \geq F_{AD} \cdot u_{AD} \cdot \Delta t$, then $F_{AD} \cdot u_{AD} \cdot \Delta t = F_A \cdot u_{AD} \cdot \Delta t$. On the other hand, if $F_D \cdot \Delta x_D < F_{AD} \cdot u_{AD} \cdot \Delta t$, then $F_{AD} \cdot u_{AD} \cdot \Delta t = F_D \cdot \Delta x_D$. Subscripts A, D, and AD means values at accepter cell, donor cell, and interface, respectively. In the case of $(1 - F_D) \cdot \Delta x_D < (1 - F_{AD}) \cdot u_{AD} \cdot \Delta t$, which means the more void fraction is to be transferred during calculation, $F_{AD} \cdot u_{AD} \cdot \Delta t$ has to be modified by adding $[(1 - F_{AD}) \cdot u_{AD} \cdot \Delta t - (1 - F_D) \cdot \Delta x_D]$. This procedure can be expressed using the following formula considering one more cell neighboring the donor cell :

$$(u_{AD} F_{AD}) \cdot \Delta t = \text{sgn}(u_{AD}) \cdot \min[F_{AD} \cdot | u_{AD} \cdot \Delta t| + CF, \ F_D \Delta x_D] \quad (6)$$

$$CF = \max[(\max(F_D, F_{DM}, 0.1) - F_{AD}) \cdot |u_{AD} \cdot \Delta t| - (\max(F_D, F_{DM}, 0.1) - F_D) \Delta x_D, \ 0] \quad (7)$$

where F_{DM} is the volume fraction of the upstream cell of donor cell.

The calculated $F_{AD} \cdot u_{AD} \cdot \Delta t$ at each face of a control volume is to be substituted in Eq. (5), and then volume fraction of fluid can be determined. Since the calculation for the VOF procedure is based on the explicit concept, the new location of the free surface has to be determined using the velocities at *t-stage* of elapsed time before going into the velocity calculations at $t + \Delta t$-*stage* (Hirt et al., 1981 ; Nichols et al., 1971). The time step is determined by follows.

$$\Delta t < MIN\left[\frac{\delta x_i}{u_{i,j,k}}, \ \frac{\delta y_j}{v_{i,j,k}}, \ \frac{\delta z_k}{w_{i,j,k}}\right] \quad (8)$$

This is to make sure that the volume fraction can not move through more than one cell in one time step, so Eq. (8) is applied only during the mold filling (Hirt et al., 1981).

2.2.2 Treatment of phase change

When a material changes its phase, it evolves latent heat. And the evolution of latent heat makes the temperature variation slow, as if heat

transfer occurs in a material of high specific heat. This is the principle of the Equivalent Specific Heat method (Ohnaka, 1984), which is adopted in the present combined method with modification. Thus the latent heat release is evaluated as an increment of specific heat in the Equivalent Specific Heat method. So the temperature during phase change is calculated by the Equivalent Specific Heat method, and then the solid fraction (f_s) is determined by temperature using $f_s = (T_{liq} - T)/(T_{liq} - T_{sol})$, and finally the solidified region is identified by control volumes with solid fraction of 1. It is called a solidified cell. The phase change process introduces a source term in the energy equation. This term is given by

$$S = \frac{\rho}{c_p} \frac{\partial \Delta H}{\partial t} = \frac{\rho}{c_p} \frac{\partial \Delta H}{\partial T} \frac{\partial T}{\partial t}$$ (9)

where $\Delta H = L \cdot f_s$, $f_s = \dfrac{T_{liq} - T}{T_{liq} - T_{sol}}$

and is linearized as:

$$\Rightarrow \frac{\rho}{c_p} \frac{L}{T_{liq} - T_{sol}} \frac{1}{\Delta t}(T_p^{old} - T_p) = S_c + S_p \cdot T_p$$ (10)

A careful treatment is required when the temperature drops across the liquidus or the solidus line, because the latent heat evolves only when the phase change occurs $(T_{sol} < T < T_{liq})$. The Equivalent Specific Heat method does not consider the variation of latent heat evolution during iterations within a time step, but modifies the final temperature field to minimize the error caused by the temperature variation crossing the liquidus or solidus line (Ohnaka, 1984). Another method to treat the phase change problem is the Enthalpy method (Bennon et al., 1987 ; Lee et al., 1995). It considers the variation of latent heat evolution during the iteration and is known to give better solution, but when the temperature is to be used during calculation, the enthalpies need to be converted into temperatures. The Equivalent Specific Heat method used in the present study takes the latent heat release during iteration into consideration and does not include converting process (enthalpy ↔ temperature); for solidification, if $T_p < T_{liq} < T_p^{old}$, then T_p^{old} is to be replaced by T_{liq}, and if $T_p < T_{sol} < T_p^{old}$, then T_p is to be replaced by T_{sol}. This process has to be repeated until the converged temperature profiles are gained. They are to make sure that the value of the solid fraction (f_s) or the liquid fraction $(f_l = 1 - f_s)$ exists between 0 and 1 as in the Enthalpy method. The schematics are shown in Fig. 2(a). When the temperature drops across a liquidus line, the decreasing rate of temperature is changed and slower. When the temperature drops across a solidus line, the decreasing rate of temperature is changed again and faster. Finally, the unsteady term in the energy equation becomes

$$\rho \frac{(T_p - T_p^{old})}{\Delta t} \Delta V + \frac{\rho}{c_p} \frac{L}{T_{liq} - T_{sol}} \frac{(T_p - T_p^{old})}{\Delta t} \Delta V$$

$$= \frac{\rho}{c_p}\left(c_p + \frac{L}{T_{liq} - T_{sol}}\right) \frac{(T_p - T_p^{old})}{\Delta t} \Delta V$$ (11)

$$= \frac{\rho}{c_p}\left(c_p + \frac{L}{T_{liq} - T_{sol}} \frac{f(T, T^{old})}{T_p - T_p^{old}}\right) \frac{T_p - T_p^{old}}{\Delta t}$$

where

$$f(T, T^{old}) = \begin{cases} T - T_{liq} & : T < T_{liq} \text{ and } T^{old} > T_{liq} \\ T - T^{old} & : T > T_{sol} \text{ and } T^{old} < T_{liq} \\ T_{sol} - T^{old} & : T < T_{sol} \text{ and } T^{old} > T_{sol} \end{cases}$$

$c_p + L/(T_{liq} - T_{sol})$ in the 2nd line of Eq. (11) is a new specific heat in the conventional Equivalent Specific Heat method. While this new specific heat is not updated during iterations within a time step and the temperature field is corrected in the end of iterations in the conventional method,
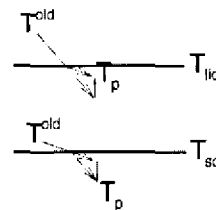
(a) Temperature variation across liquidus or solidus line
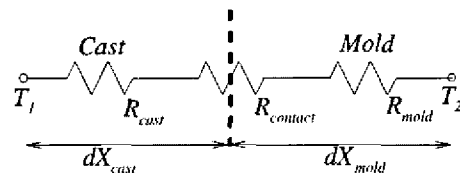
(b) Boundary between cast and mold

Fig. 2 Boundary examples for heat transfer in casting process

this value is updated per iteration and the temperature field needs not to be corrected in the end of calculation within a time step in the new method by implementing the function f as in the 3rd line in Eq. (11). In the case of pure metal $(T_{sol}=T_{liq})$, $T_{sol}-T_{liq}$ is assumed to be a small value, since there isn't a mushy zone during phase change of a pure material.

2.2.3 Treatment of boundary conditions

Another key item in the precise analysis of the casting process is the treatment of the boundary conditions on the free surface. The basic idea in the SIMPLE algorithm is that the pressure gradient drives the velocity (Patankar, 1980), and the normal stress condition describes the pressure on the free surface as the combination of velocity gradients (Nichols et al., 1971). In the light of this concept, since the normal stress condition that explains the pressure on the free surface as the equivalence of the stresses (expressed in terms of velocity vectors), it is easily combined with the SIMPLE algorithm as a free surface boundary condition. As one example, let's consider again the situation in Fig. 1(b).

$$a_s v_s = \sum a_{nb} v_{nb} + b + (p_s - p_P) A \qquad (12)$$

To solve Eq. (12), the pressure p_P is needed and it can be attained using the normal stress condition. From Eq. (3), since i indicates the y-direction in Fig. 1(c), the following differentiation and discretized equations are given.

$$2\mu \frac{\partial v}{\partial y} = p_P \Rightarrow p_P = 2\mu \frac{v_n - v_s}{\Delta y_P} \qquad (13)$$

v_n and Δy_P can be determined using the continuity equation and the volume fraction of fluid in free surface cell P by applying calculated control volume $(\Delta x \cdot \Delta y \cdot \Delta z \cdot F)$, which is another practical way of the VOF method. To minimize the calculation time, atmospheric pressure (reference pressure) is assumed on the free surface, when more than two control volume faces are open to the empty cell or when two control volume faces open to the empty cells are facing each other (Hirt et al., 1968). So the pressure on the free surface boundary is to be calculated by the normal stress condition and needs not to be

corrected in SIMPLE(R) procedure like the pressure on solid boundary. Now, another difficult problem in free surface boundaries is the velocity that is parallel to the free surface like the velocity u_w or w_b in Fig. 1(b), (c). u_w and w_b are expressed as follows.

$$a_w u_w = a_e u_e + a_{ww} u_{ww} + a_{wn} u_{wn} + a_{ws} u_{ws} \\ + a_{wt} u_{wt} + a_{wb} u_{wb} + b + (p_w - p_P) A \qquad (14)$$

$$a_b w_b = a_{be} w_{be} + a_{bw} w_{bw} + a_{bn} w_{bn} + a_{bs} w_{bs} \\ + a_t w_t + a_{bb} w_{bb} + b + (p_B - p_P) A \qquad (15)$$

Now, we need to know u_{wn} and w_{bn} to make Eq. (14), (15) meaningful with the equations for the filling process. As can be seen from Fig. 1(b), (c), u_{wn} and w_{bn} are not the velocities in the fluid region. Though some workers applied the symmetric boundary conditions on the free surface (Lee et al., 1995), the tangential stress condition, which means 0-shear stress on the free surface, is adopted in this study. Now when the tangential stress condition is applied? In the case of 2-dimensional problem, thousands of free surface inclinations are possible. In the 3-dimensional case, there are normal vector (to the free surface) and the tangential plane, and it's much more complicated to calculate their mathematical quantities. As it is required enormous computing time, we simplified the cases of free surface shape into 2 cases in the present work as is done by others (Hong et al., 2001; Chen et al., 1995; Maronnier et al., 2003). For the 2-dimensional case, one is the free surface close to 0° (or 90°) and the other is that close to 45° (or −45°). The same simplification was made in 3-dimensional case. Thus the calculations are made according to the following 2 cases.

Case I   0°(0°, 90°, 180°, 270o)
Case II   45°(45°, 135°, 225°, 315°)

Any free surface cell surrounded by the facing empty cells and (or) facing fluid cells (including both fully and partially fluid cells) with normal direction open to the empty cell is classified as Case I. Otherwise, it belongs to Case II. When the free surface cells are located next to each other in x_i direction and the empty cells are also located

parallel to the free surface cells, the tangential stress condition is applied and the free surfaces in this case are classified into Case I.

Again in Fig. 1(c), the free surface shape is a case I and Eq. (4) gives following condition.

$$\tau_{yx}=\tau_{yz}=0 \qquad (16)$$

From Eq. (16), $\tau_{yx}=0$ is applied to attain u_{wn}, and $\tau_{yz}=0$ is applied to attain wbn like follows.

$$\frac{\partial v}{\partial x}+\frac{\partial u}{\partial y}=0 \Rightarrow u_{wn}=u_w+\frac{\Delta y_{w-wn}}{\Delta x_{n-nw}}(v_n-v_{nw})$$
$$\frac{\partial v}{\partial z}+\frac{\partial w}{\partial y}=0 \Rightarrow w_{bn}=w_b+\frac{\Delta y_{b-bn}}{\Delta z_{n-nb}}(v_n-v_{nb}) \qquad (17)$$

Finally, together with the no-slip wall condition on the solid boundaries, all the boundary conditions are implemented clearly.

Concerning the heat transfer between mold-cast or cast-inner air or mold-outer air, it can be calculated by composing a resistance circuit (Mills, 1992). As one example, the resistance circuit is shown in Fig. 2(b) for a mold-cast boundary. The contact resistance $R_{contact}$ is affected by solidification shrinkage, radiation heat transfer, temperature variation in each region etc in the casting processes. So the effective heat transfer coefficient between mold and casting is given as:

$$h_{eff}=\frac{1}{R}=\frac{1}{R_{cast}+R_{contact}+R_{mold}}$$
$$=\frac{1}{\dfrac{dx_{cast}}{k_{cast}}+\dfrac{1}{h_{radiation}+h_{gap}+\cdots}+\dfrac{dX_{mold}}{k_{mold}}} \qquad (18)$$

2.3 Turbulent modeling

In many cases, the filling process in the casting process is liable to be turbulent flow. To consider the turbulent effect, the Turbulent Viscosity (Eddy Viscosity) was applied directly to the Navier-Stokes equations without additional differential equations. The runner system was modeled as a non-circular duct flow and the rectangular cavity zone was modeled as a channel flow between parallel plates. So the following formulas were adopted to calculate the Turbulent Viscosity.

$$\frac{1}{\varLambda^{1/2}}=2.0\log_{10}(0.64\text{Re}_{D_h}\varLambda^{1/2})-0.8 \quad Duct\ Flow$$
$$\qquad (19)$$
$$\frac{1}{\varLambda^{1/2}}=2.0\log_{10}(\text{Re}_{D_h}\varLambda^{1/2})-1.19 \quad Channel\ Flow$$

D_h's in Eq. (19) are the hydraulic diameters and $\varLambda=4\cdot C_f=4\cdot(2\tau_w/\rho u_{av})$ can be used. Though Zero-Equation model for turbulent flow is very useful in terms of saving computation time, the $\kappa-\varepsilon$ model or the Reynolds stress model is to be implemented as a future work for the precise solution and wide application. Since the turbulent thermal conductivity is assumed to be negligible when the Prandtl number is very small, the temperature profiles can be computed without any further assumptions in the case of molten metal (Pr<0.1). (Hetu et al., 1999 ; White, 1991)

2.4 Details of the physical situation

The mold shape and dimensions used in the present calculation is shown in Fig. 3 along with the properties of materials in Table 2. This is a famous benchmark test from the 7th Conference on Modeling of Casting, Welding, and Advanced Solidification Process (MCWASP VII). The filling proceeded as much as the rate that the
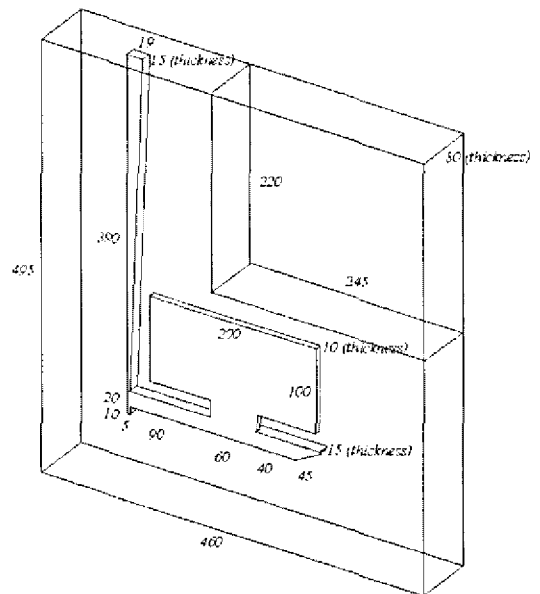

Fig. 3 Geometirc model used in the present study

Table 2 Material properties used in mold filling and solidification

Material (Latent Heat : J/kg)	Property name	Conductivity (k : W/mK)	Specific Heat (c_p : J/kgK)	Density (ρ : kg/m^3)	Viscosity (μ : kg/m s)
Pure Aluminium (293,820)	Liquid Phase	90.0	1080.0	2561.0	0.01024
	Solid Phase	210.0	1202.0	2571.0	1E30
No Baked Sand		0.6061	1128.6	1500.0	1E30

Table 3 Property values used for phase front tracking

Property name	Region Mold part	Cast part
Conductivity (J/m sec K)	—	41.9
Specific Heat (J/kg K)	—	627.9
Density (kg/m^3)	—	7000
Initial Temperature/Liquidus Temperature (K)	293/—	1753/1753
Latent Heat (J/kg)	—	272093.0
Contact Heat Transfer Coefficient (J/m^2 sec K)	—	2093.0

height of molten metal level in the pouring basin could be kept constant (4 cm). The pouring basin was not included in the numerical model of the present study, but the inlet condition (pressure) was applied using the Bernoulli's Equation (Mills, 1992 ; White, 1991).

$$p_{inlet} = p_{reference} + \rho g \Delta h - \frac{1}{2} \rho v_{inlet}^2 \qquad (20)$$

where Δh is the level of molten metal in the pouring basin.

Initial molten metal temperature was around 998°K in the experiment. While the mold was assumed to be at atmospheric temperature in the numerical calculation its value was not given in the experimental conditions. Heat transfer occurred via molten metal -> mold -> air. The contact thermal resistance between mold and cast was assumed to be constant and fixed to 1/2000 W/m²K based on δ_{gap}/k_{gas} of the thermal resistance value. But, for a precise analysis of heat transfer through the mold-cast boundary, more complicated mathematical formulas and data have to be used (Griffiths, 1999). The properties of pure Aluminum and sand (mold) used in the numerical calculation were taken mostly from the reference on the experiment (Sirrell et al., 1995).

3. Results

3.1 Computational details

A non-uniform grid comprising of (75, 72, 25) control volumes was used. The mesh was finer in the fluid region, while it was coarser in the mold region. The mesh spacing used in the present study have the maximum edge length of 12.0×10^{-3} m and the minimum 1.25×10^{-3} m.

3.2 Validation of a numerical model

We present a comparison between exact solution and simulation results to verify the numerical model for the phase change process. The exact solution was referred to the Garcia, et al.'s formula in the text (Ohnaka, 1984) and it is

$$x = -2a_s a\phi^2 + 2\phi\sqrt{a_s^2 a^2 \phi^2 + a_s t}$$

$$a = \frac{\rho_s C_{ps}}{\sqrt{\pi}\phi \exp(\phi)[M + erf(\phi^2)]h}$$

$$\frac{\exp(-\phi^2)}{M + erf(\phi)} = \frac{m(T_p - T_f)\exp(-n^2\phi^2)}{(T_f - T_{m0})[1 - erf(n\phi)]} + \frac{\sqrt{\pi}L\phi}{C_{ps}(T_f - T_{m0})} \qquad (21)$$

$$M = \left(\frac{k_s \rho_s C_{ps}}{k_m \rho_m C_{pm}}\right)^{1/2}, \ m = \left(\frac{k_s \rho_s C_{ps}}{k_l \rho_l C_{pl}}\right)^{1/2}, \ n = \left(\frac{a_s}{a_l}\right)^{1/2}$$
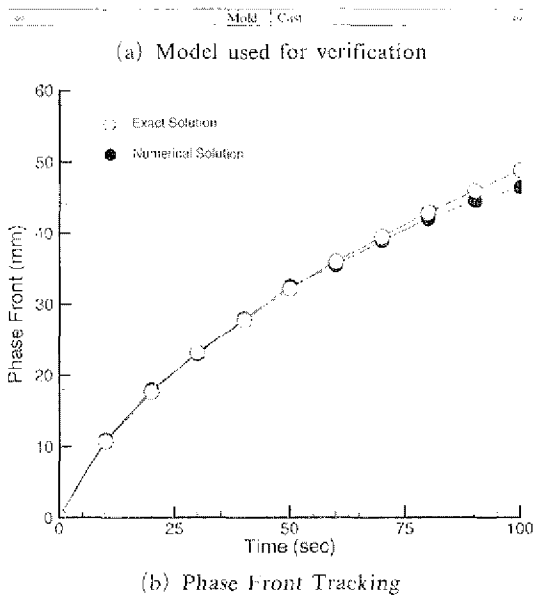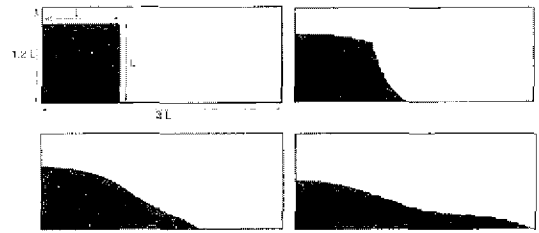
where $a = k/\rho c_p$, T_{m0} is the temperature at the

(a) Model used for verification

(b) Phase Front Tracking

Fig. 4 Verifications for the present phase change front tracking model

(a) Successive collapsing of a water column

(b) Front position of water with respect to time

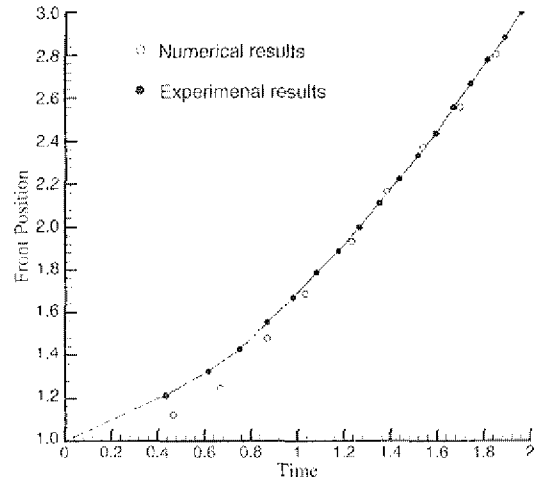**Fig. 5** Verifications for the present free surface front tracking model

interface of mold and cast, L the Latent Heat of a material, h the heat transfer coefficient at the interface of mold and cast, T_b the initial temperature, and T_f the temperature at the interface of phase change.

Figure 4(a) shows a one-dimensional semi-infinite solidification model (constant mold temperature) and the thermal properties are shown in Table 2. Since the infinite length is difficult to simulate numerically, a long length was used and the end edge was assumed to be adiabatic. Figure 4(b) shows the results. In this figure, the ordinate is the location of the phase front and the abscissa is the elapsed time. The gray circles represent the exact solutions from Eq. (21), and the black circles the numerical results. The two sets of results are in good agreement : the differences are due to the finite length used in the numerical analysis. The phase front moves faster in the early stage of solidification than in the middle and late stages, and its moving rate becomes slow in the late stage of solidification.

For the validation of the free surface tracking, a broken dam experiment was referred (Hetu et al., 1999). Figure 5(a) shows the dimensions and successive collapsing process of a water column.

Figure 5(b) shows the location of front of a collapsed water column with respect to the elapsed time. The abscissa is the elapsed time and the ordinate is the front position of a collapsed water column. As can be seen from Fig. 5(b), the experiment and the simulation by the present method provided enough agreement.

After these validations, the present combined numerical model was applied to a casting process that was a bench mark problem in the 7th MCWASP (Sirrell et al., 1995).

3.3 Filling process

If a cast is not long (or deep) enough in lateral direction or not axi-symmetrical, it should be modeled three dimensionally. That is, except for a few cases, the two dimensional models are good for developing theories or theoretical studies rather than practical applications. To see the differences of the two dimensional and three dimen-

sional analyses, the two dimensional results were shown together with the three dimensional results.

Figure 6 shows four sets of results for mold filling : three experimental test results (Sirrell et al., 1995), numerical results from a two dimensional analysis, numerical results from the literature (Hetu et al., 1999), and numerical results by the present method. Three experimental tests are very famous Bench Mark test done in the Proceedings of the 7th International Conference in Modeling of Casting, Welding and Advanced Solidification Processes. Concerning the two dimensional analysis, $w=0$ and $\partial/\partial z=0$ were assumed. The boundary conditions used in the two dimensional analysis were identical to those of the three dimensional analysis. In Fig. 6(a) at 0.75 sec, the four sets of results do not match exactly. At this instant, though three test results are not exactly identical, the melt entering the rectangular mold cavity is clearly going toward

right in the experimental results. While the melt is entering the cavity with the same direction to the tests in the three dimensional numerical results of J. Hetu et al's and present method, the direction is rather reversed in the two-dimensional analysis. This behavior is attributed to the exaggerated effect of inertia force in the two-dimensional analysis due to the lack of z-directional effect (thickness, one of the three dimensional effects), i.e. the intensity of the returning flow from the dead end of flow path is much stronger than what it should be in the real situation. At 1.00 sec in Fig. 6(b), the free surface level in the mold cavity is higher in the right region than the left region. All of experimental and numerical results show this tendency, but the two dimensional solution has wavier surface than the experiment or the three dimensional numerical results, again due to the large inertia force. The differences between three dimensional and two-dimensional results
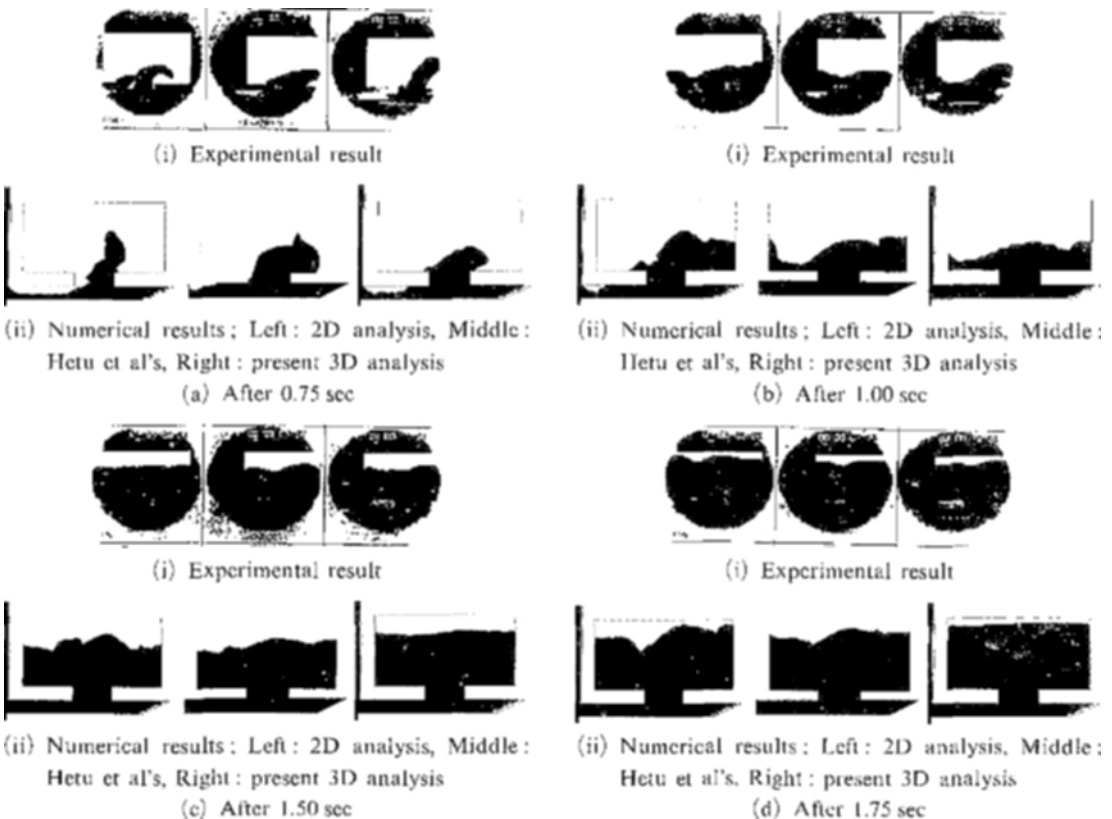

(i) Experimental result

(ii) Numerical results ; Left : 2D analysis, Middle : Hetu et al's, Right : present 3D analysis

(a) After 0.75 sec

(i) Experimental result

(ii) Numerical results ; Left : 2D analysis, Middle : Hetu et al's, Right : present 3D analysis

(b) After 1.00 sec

(i) Experimental result

(ii) Numerical results : Left : 2D analysis, Middle : Hetu et al's, Right : present 3D analysis

(c) After 1.50 sec

(i) Experimental result

(ii) Numerical results : Left : 2D analysis, Middle : Hetu et al's, Right : present 3D analysis

(d) After 1.75 sec

Fig. 6   Sequences of mold filling process

become more and more pronounced as filling proceeds. In the experiments, the free surface starts leveling off at 1.50 sec, as can be seen in Fig. 6(c). Such tendency was also seen in the three-dimensional numerical models, while the wavy surface still prevails in the two-dimensional simplified model. Concerning the last region of filling, it is easy to see that the region will be formed along the top boundary, as predicted by the present three-dimensional results as well as the experimental results in Fig. 6(d). The two-dimensional analysis, however, results the different region of final filling; the region is likely in the right (or left) upper part of the mold cavity due to the wavy surface. J. Hetu et al's result shows a little wavier free surface than that of experiment. It can happen when the intensity of convection is over-evaluated comparing to the diffusion. In the process of designing a mold (including a riser), a number of factors can be considered through the simulation to prevent the defects in the casting process and to minimize the waste of time and money caused by the trial and error method. Since

the present three-dimensional numerical model is based on the SIMPLER algorithm with the power law scheme employed, the effect of diffusion and convection is accurately evaluated as well as the three dimensional effect. Thus the present three-dimensional numerical model for the casting processes is appropriate for the simulation of mold filling process.

3.4 Solidification process

Figure 7 shows the successive temperature profile variations in the cast and mold comparing the present results to the two-dimensional results. Both the solidification rate and the final region of solidification appeared differently in the present three dimensional and simplified two dimensional numerical analyses. To consider the heat loss through the lateral mold in the two dimensional analysis, $q_{loss} = h_{contact}(T_p - T_{mold})$ were assumed at every grid point in the cast zone. T_p represents the grid temperature and T_{mold} is assumed to have constant value identical to the initial mold temperature. Just after completion

(a) Just after completion of filling ;
Right : 3D analysis, Left : 2D analysis

(b) At 10% solidification fraction ;
Right : 3D analysis, Left : 2D analysis

(c) At 30% solidification fraction ;
Right : 3D analysis, Left : 2D analysis

(d) At 90% solidification fraction ;
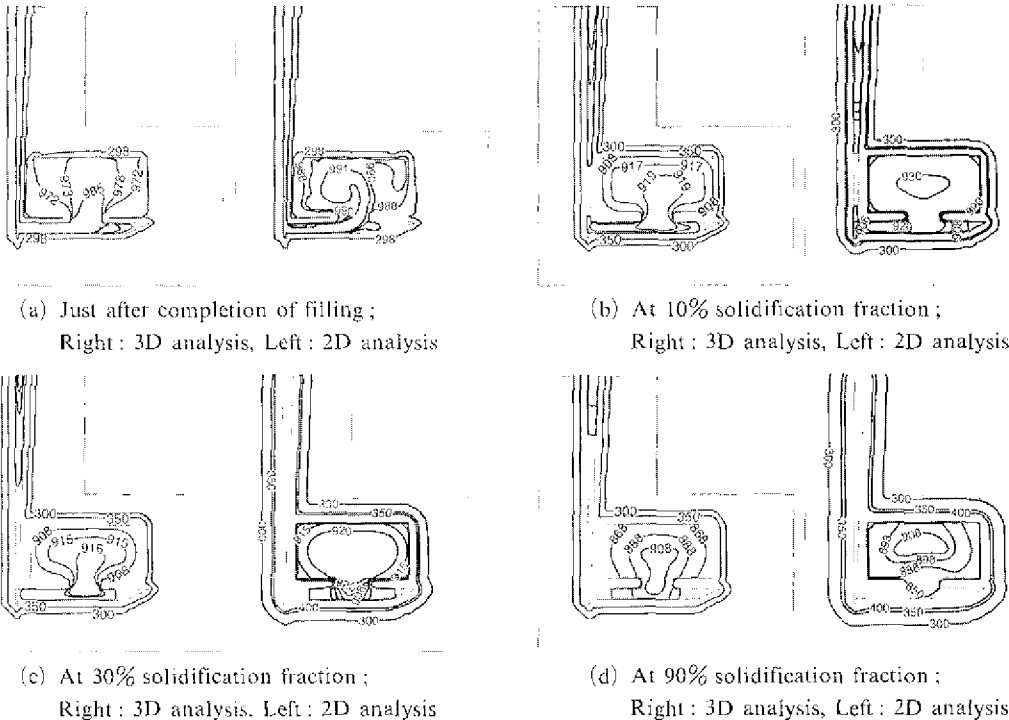Right : 3D analysis, Left : 2D analysis

Fig. 7 Sequences of solidification process

of filling (Fig. 7(a)), the mold temperature is almost its initial value without much change due to the short elapsed time for filling and the low thermal conductivity of cast sands. The melt temperature, however, is much lower than the initial molten metal temperature with the bottom corners of mold cavity the lowest, due to the cooling during filling. Not only the heat transfer during filling but also the residual flow affect the early stage of solidification, and the details for residual flow are available in the reference (Lee et al., 1999). In the three dimensional numerical results in Fig. 7(b) and (c) (10% and 30% solidification fraction respectively), the solidification occurs along the whole boundaries between mold and casting, and the phase change interface proceeds toward the lower center of rectangular cast (near gate). But, in the two dimensional results, the phase change interface moves toward the center of rectangular cavity and the temperature in the cast zone changes slower than that of three dimensional results because the thermal inertia of mold was not properly calculated in the two dimensional analysis. As a result, the predicted final solidification region in the three dimensional result is the lower center of rectangular cavity, while it is the center of cast in the two dimensional result, as can be seen in Fig. 7(d) of 90% solidification fraction. The elapsed times for the completion of solidification were 64.8 sec and 271.8 sec in the three dimensional and two-dimensional analyses, respectively (average solidification time was 63 sec in the experiments (Sirrell et al., 1995)). The fundamental reason for such differences is the cooling capacity of the mold. A mold can be a heat sink for the cast as well as a medium to transfer heat from the cast to air or coolant. And it is very hard to estimate the heat loss in the lateral direction using a two dimensional model not only in cast zone but also in mold zone. Since the cooling in z-direction occurs in $\pm z$ directions, we may want to set q_{loss} as $2 \cdot h_{contact}(T_p - T_{mold})$. But it won't improve the prediction by a two dimensional model. These results indicate that the three-dimensional model is essential to obtain accurate quantitative results. Only a three dimensional model can form

the basis of a simulation tool for designing castings.

Figure 8 shows the cooling histories from the different locations in the cast: A(215 mm, 140 mm), B(215 mm, 180 mm), C(215 mm, 220 mm), D(305 mm, 140 mm), E(305 mm, 220 mm), F (125 mm, 140 mm), G(125 mm, 220 mm). As predicted by the present numerical model, the solidification occurred first at each edge (D, E, F, G) and the final solidification occurred at A where the lower center of mold cavity. While the temperatures were kept constant during phase change in the experiment, they dropped slightly in the numerical result. It's because that 908°K and 933.4°K were used in the calculation for the solidus and liquidus line of pure Aluminum as the reference recommended (Sirrell et al., 1995). But in the real situation, the temperature should be kept constant during phase change if the ma-
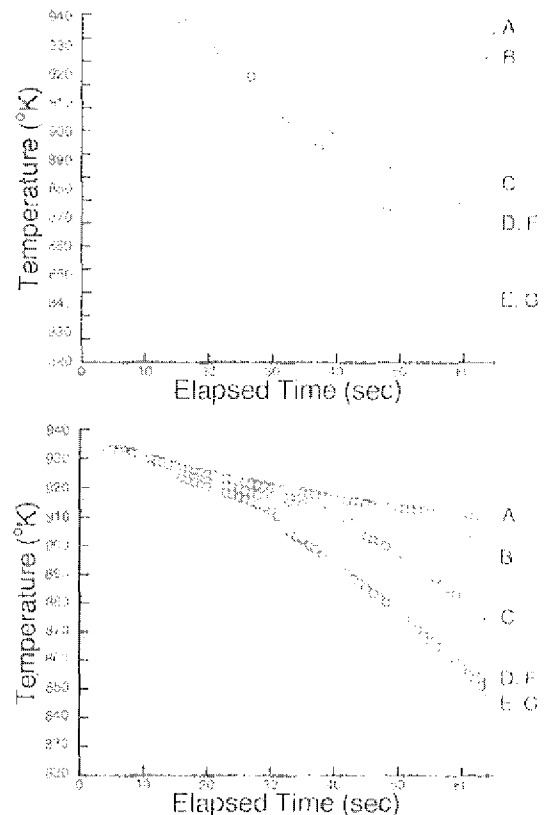

Fig. 8 Cooling curves from different locations in the cast (Left: Experimental result, Right: Numerical result)

terial is 100% pure (it was 99.999% pure Al in the experiment). The constant $h_{contact}$ (=2000 W/m^{2}K) assumption also caused gap between the experimental and numerical results. Though the cooling curves did not match exactly, solidification at each location proceeded with same manner resulting small differences.

4. Conclusion

A new combined algorithm of the SIMPLER, VOF, and Equivalent Specific Heat method has been developed and compared both to the exact solutions of phase front tracking and to the experimental results of a collapsed water column for validation. The new combined algorithm was also applied to the mold filling and solidification process with the results compared to the experimental results and other numerical results. As a result of analysis, the following conclusions were obtained.

(1) The present numerical model developed through the new combined algorithm was proven to be very successful through the verification of a phase change front tracking of semi-infinite cast-mold system and the free surface behavior of a broken dam.

(2) The present three dimensional numerical model was able to predict the mold filling and solidification processes accurately with the three dimensional effects and the combined effect of diffusion and convection intensities properly considered.

(3) The locations of free surface and phase change front in the filling and solidification processes of rectangular mold could be tracked exactly by the present numerical model, which are important factors for designing a mold.

References

Beckermann, C. and Viskanta, R., 1993, "Mathematical Modeling of Transport Phenomena during Alloy Solidification," *ASME Appl. Mech. Rev.*, Vol. 46, No. 1, pp. 1∼27.

Bennon, W. D. and Incropera, F. P., 1987, "A Continuum Model for Momentum, Heat and Species Transport in Binary Solid-Liquid Phase Change System — I. Model Formulation," *Int. J. Heat Mass Transfer*, Vol. 30, No. 10, pp. 2161∼2170.

Bennon, W. D. and Incropera, F. P., 1987, "A Continuum Model for Momentum, Heat and Species Transport in Binary Solid-Liquid Phase Change System — II. Application to Solidification in a Rectangular Cavity," *Int. J. Heat Mass Transfer*, Vol. 30, No. 10, pp. 2171∼2187.

Chen, S., Johnson, D. B. and Raad, P. E., 1995, "Velocity Boundary Conditions for the Simulation of Free Surface Fluid Flow," *J. Comput. Phys.*, Vol. 116, pp. 262∼276.

Griffiths, W. D., 1999, "The Heat Transfer Coefficient during the Unidirectional Solidification of an Al-Si Alloy Casting," *Met. & Mater. Trans. B*, Vol. 30, pp. 473∼482.

Harlow, F. H. and Amsden, A. A., 1971, "Numerical fluid Dynamics Calculation Method for all Flow Speeds," *J. Comput. Phys.*, Vol. 8, p. 197.

Hirt, C. W. and Nichols, B. D., 1981, "Volume of Fluid (VOF) Method for the Dynamics of Free Boundaries," *J. Comput. Phys.*, Vol. 39, pp. 201∼225.

Hirt, C. W. and Shannon, J. P., 1968, "Free Surface Stress Conditions for Incompressible Flow Calculations," *J. Comput. Phys.*, Vol. 2, pp. 403∼411.

Hetu, J. and Ilica, F., 1999, "A Finite Element Method for Casting Simulation," *Numerical Heat Transfer A*, Vol. 36, pp. 657∼697.

Hong C. P., Lee, S. Y. and Song, K., 2001, "Development of a New Simulation Method of Mold Filling Based on a Body Fitted Coordinate System," *ISIJ International*, Vol. 42, No. 9, pp. 999∼1005.

Hwang, W. S. and Stoehr, R. A., 1983, "Fluid Flow Modeling for Computer Aided Design of Castings," *Journal of Metals, Oct.*, pp. 22∼29.

Koo, E. M., Mok, J., Lee, J. H., Hong, C. P. and Yoon, Y. S., 2001, "Numerical Analysis of Fluid Flow of Molten Metal and Solidification Characteristics in the Casting Process under Centrifugal Force," *J. Kor. Inst. Met. & Mater.*,

Vol. 39, No. 3, pp. 367~373.

Lee, J. and Hwang, K. Y., 1995, "Effects of Density Change and Cooling Rate on Heat Transfer and Thermal Stress During Vertical Solidification Process," *KSME*, Vol. 19, No. 4, pp. 1095~1101.

Lee, J., Mok, J. and Hong, C.P., 1999, "Straightforward Numerical Analysis of Casting Process in a Rectangular Mold : From Filling To Solidification," *ISIJ International*, Vol. 39, No. 12, pp. 1252~1261.

Lee, K. H., Mok, J. and Lee, J., 2001, "The Effect of Thermosolutal Convection on Macrosegregation during Alloy Solidification," *KSME*, Vol. 25, No. 10, pp. 1337~1345.

Mampaey, F. A. and Xu, Z. A., 1995, "Simulation and Experimental Validation of Mold Filling," *Proceedings of Modeling of Casting, Welding and Advanced Solidification Processes-VII*, pp. 3~14.

Maronnier, V., Picasso, M. and Rappaz, J., 2003, "Numerical Simulation of Three-Dimensional Free Surface Flow," *Int. J. Numer. Meth. Fluids*, Vol. 42, pp. 697~716.

Mills, A. F., 1992, Heat Transfer, IRWIN, Boston.

Nichols, B. D. and Hirt, C. W., 1971, "Improved Free Surface Boundary Conditions for Numerical Incompressible Flow Calculations," J. Comput. Phys., Vol. 8, pp. 434~448.

Ohnaka, I., 1984, *Computer Aided Heat Transfer and Solidification (Application to Casting Process)*, Maruzen, Japan.

Patanker, S., 1980, *Numerical Heat Transfer and Fluid Flow*, Hemisphere, Washington.

Sirrell, B., Holliday, M. and Campbell, J., 1995, "the Bench Mark Test 1995," *Modeling of Modeling of Casting, Welding, and Advanced Solidification Processes VII*, pp. 915~933.

White, F. M., 1991, Viscous Fluid Flow, McGrawHill, New York.